International Journal of Latest Research in Science and Technology
Volume 3, Issue 2: Page No.73-79 ,March-April, 2014
https://www.mnkpublication.com/journal/ijlrst/index.php

ISSN (Online):2278-5299

SOLUTION-BASED GROWTH OF ZnO NANOROD ARRAYS WITH SZO FILMS AND THEIR APPLICATION IN DYE-SENSITIZED SOLAR CELL

[1,3]I. Saurdi, [1,2]M. Rusop

[1]NANO-ElecTronic Centre, Faculty of Electrical Engineering, UniversitiTeknologiMARA,
40450 Shah Alam, Selangor, Malaysia
[2]NANO-SciTech Centre, Institute of Science, UniversitiTeknologi MARA,
40450 Shah Alam, Selangor, Malaysia
[3]Facuty of Electrical Engineering,
UiTM SarawakKampus Kota SamarahanJalanMeranek, Sarawak

Abstract*- The Sn-doped ZnO thin films were deposited on glass and ITO substrates by sol gel spin coating technique. The structural, optical and electrical properties of Sn-doped ZnO thin films were studied and discussed. The Sn-doped ZnO thin film particle sizes were decreased whenever the doping concentration increased. Furthermore, high average transmittance of 96% in visible region and resistivity 7.7 x 10^2 Ω.cm were obtained with 2 at% Sn-doped ZnO as well as aligned ZnO nanorod arrays with large surface area were grown on 2 at.% Sn-doped ZnO film by using sol gel immersion ultrasonic assisted. Besides that, the optical properties of grown aligned ZnO nanorod arrays shows high transmittance at visible region that favorable for dye-sensitized solar cell. At 2 at.% Sn-doped film ZnO nanorod had higher IPEC due to high light scattering and enhance the photogenaration from absorbed dye. Therefore, dye sensitized solar cell at 2.0 at.% Sn-doped ZnO thin film with ZnO Nanorod arrays have an improved of current density, open circuit voltage, fill factor, and conversion efficiency.

Keywords – Zinc oxide, Sn dopant, Nanorod, Dye Sensitized, Solar Cell

I. INTRODUCTION

Nowadays, one-dimensional ZnO semiconductor has been widely studied due to it great advantageous nanostructures, such as nanosheet, nanowiress (NWs) and nanoflowers that have attracted much attention for various applications arising from their unique properties [1]. Zinc oxide (ZnO) is a wide-bandgap II-VI compound with a direct bandgap of 3.37 eV and 60m eV of free-exciton excitation energy at room temperature. It could be synthesized in many forms of nanostructures by simple and low-cost techniques such as sol-gel and solution-based method. It has been seen that various forms of ZnO morphologies and sizes significantly contribute to the novel characteristics of the devices. Recently, many researchers have reported dye-sensitised solars (DSSCs) cell using various kinds of ZnO nanostructures [2-4], and show a significant improvement for DSSCs photovoltaic characteristics. Meanwhile, the aligned zinc oxide (ZnO) nanorod arrays nanostructures can give an extra merit on large surface area and superior carrier transport properties for DSSCs [5-6]. Besides that, the use of a lattice-matched and conducting buffer layer is a feasible way to grow nanorod and nanowire, instead of using other material such as sapphire which is insulating and expensive. Therefore, the ZnO nanorod and nanowire arrays grown on the metal doped ZnO seed layer are extensively studied. Moreover, the Sn-, Al-,Ga- and In-Doped ZnO thin films that shows high crystalline structure are reported useful for practical application on various electronic devices such as solar cells, electroluminescence displays, etc [7-9]. The metal doped ZnO can be prepared by several of techniques such as atomic layer deposition [10], chemical vapour deposition [11], sol gel [12] pulsed laser deposition [13], RF sputtering [14] and spray pyrolysis [15] etc. Among these techniques the most effective ones in term of a low cost and offering economical production is a sol gel technique.

II. EXPERIMENTAL

The Sn-doped ZnO (SZO) thin films and the aligned ZnO nanorod grown on Sn-doped ZnO seed layer were prepared and grown by sol gel immersion ultrasonic assisted.0.4M zinc acetate dehydrate, ($Zn(CH_3CO_2)_2.2H_2O$) was first dissolved in a 2-methoxyethanol-monoethanolamine (MEA) with molar ratio 1:1 at room ambient. Then appropriate amounts of Sn (tin) doping were achieved by adding tin (IV) chloride pentahydrate to the precursor solution. In order to utilize the Sn-doped ZnO thin films as a seed layer for ZnO nanorod arrays growth. There are three solutions were prepared with doped concentration of Sn/Zn=0, 1, 2 at.% respectively. Effects of the Sn-doped concentration on structural, optical and electrical properties of the Sn-doped ZnO thin films were studied. Besides that, the structural and optical properties of aligned ZnO nanorod growth on different concentrations of Sn (0, 1, 2at.%) were

Publication History
Manuscript Received : *22 April 2014*
Manuscript Accepted : *27 April 2014*
Revision Received : *29 April 2014*
Manuscript Published : *30 April 2014*

also studied as well as their electronic properties in dye sensitized solar cell. The solution was stirred and heat for 3 hours before aged for 24 hours at room ambient. The Sn-doped ZnO thin films thin films were spin-coated on glass and ITO substrates at a speed of 3000 rpm for 1 minute. Subsequently, each layer of deposited thin film was preheated in air at 150 °C to evaporate the solvent. The coating procedure was repeated a few times to increase the film thickness. After that, the thin film was finally post-heated at 500° C for 1 h in air using an electronic furnace. Corresponding to the different Sn-doped ZnO concentrations (0, 1, and 2 at.%), the obtained thin films were labeled as sample S, Sample T and Sample U, respectively. The ZnO nanorod arrays were deposited on Sn doped ZnO thin film-ITO coated glass substrates using zinc acetate solution. The zinc acetate solution was composed of the mixture of zinc acetate dihydrate, hexamethylenetetramine (HMT) and deionized (DI) water. The solution was sonicated for 30 minutes before stirred and aged for 3 hours. The growth process of ZnO nanorod arrays was conducted using water bath instrument at 95 °C. The seed layered-ITO coated glass substrates were immersed into zinc acetate solution using Schott bottles. The bottles were put inside water bath instrument for 1 hour for nanorods deposition process. After the immersion process, the samples were taken out from the bottles and dried in air for 10 minutes. Finally, the samples were annealed in air at 500^{o}C.

To fabricate DSSCs, ZnO nanorod photoanode were immersed in 0.5mM ethanolic solution of (Ru[LL'$(NCS)_2$], L=2,2'-bypyridyl-4,4'-dicarboxylic acid, L'=2,20-bypyridyl-4,4'-ditetrabutylammonium carboxylate) dye (N719) at room temperature for 24h. Pt (60 nm thick) sputtered on ITO was used as an electrochemical catalyst for the counter electrode. The substrate with ZnO nanorod electrode and dye was bonded with a sputtered counter electrode using holt-melt spacer. Sealing was accomplished by pressing the two electrodes at about 100 $^{\circ}$C a few seconds. The electrolytes were composed of 0.5 M Lil, 0.05 M I_2 and 0.5M 4-*tert*-butyl pyridine (TBP) in acetonitrile, was then introduced into the cell by capillary forces through two holes drilled in the counter electrode. Finally, the holes were covered and sealed to prevent fluid-type electrolyte leakage. The active area of the DSSC device measured using a black mask was 0.25cm^2. The fabricated DSSC of aligned ZnO Nanorod arrays were labelled as sample ZS, sample ZT, and sample ZU. The Solar simulator (Bukuh Keiki EP200), JASCO UV-VIS/NIR spectrophotometer (V-670 EX), surface profiler (Veeco Dektak 150), X-ray diffractometer (XRD, Rigaku Co., D/MAX-2000), 2 probe current-voltage (I-V) measurement (Bukuh Keiki EP-2000), field emission scanning electron microscopic (FESEM, ZEISS Supra 40VP), and energy dispersive analyser x-ray (EDX) were used to characterize the electronic, optical, structural, electrical, and surface morphology properties ZnO nanorod arrays and Sn-doped Zno thin films.

III. RESULT AND DISCUSSION

Fig. 1 shows the FESEM images of the SZO thin film and the existing of Sn dopant in Sn-doped ZnO thin film was proven by EDAX result (Fig. 1. (d)). It can be seen that the Sn-doped ZnO thin films has a flat surface morphology and uniform grain size were prepared by the sol-gel technique. Moreover, the particle size of the thin film obviously influenced by the Sn-doped concentration that changed from 36nm, 28nm, and 20nm for 0 at.%, 1 at.%, and 2.at%, respectively as estimated by using FESEM. This phenomenon might be due to substitutional doping which was attributed from different of ionic radius of Sn^{4+} ions and Zn^{2+} ion whereby the Sn^{4+} ion has the ionic radius of 0.067nm that smaller than ionic radius of Zn^{2+} (0.074nm) that retarded the growth process of ZnO Crystalization [19-20] and indicate that the Zn^{2+} is successfully substituted by Sn^{4+} at the lattice point of ZnO.

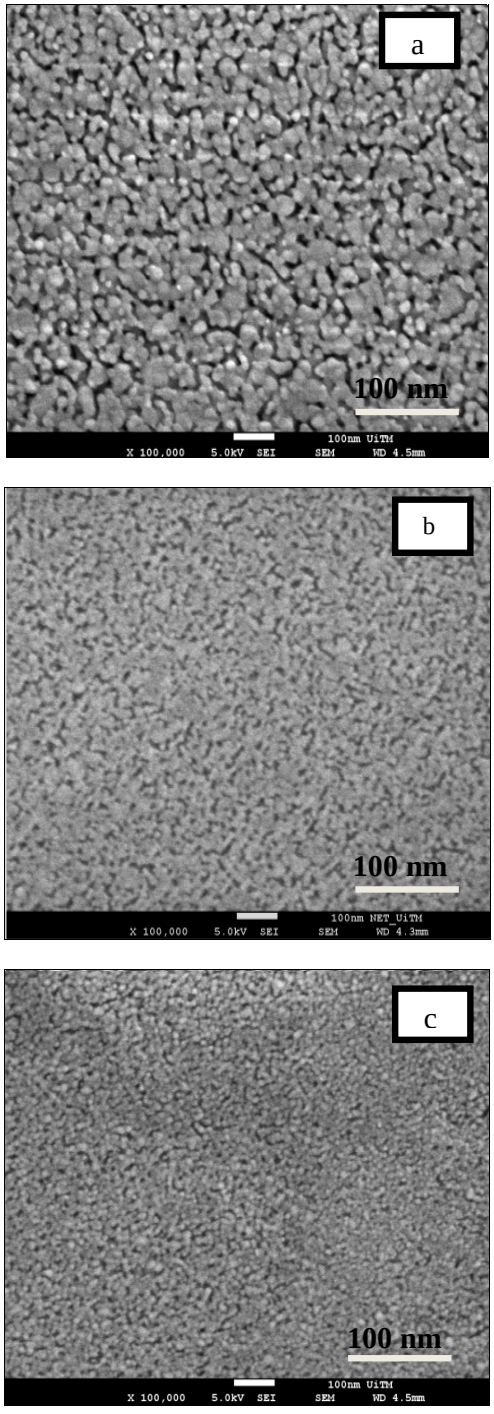

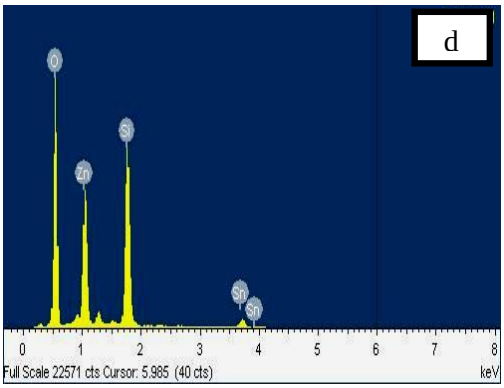

Fig.1. FESEM images of the SZO films: (a) Sample S-0at%, (b) Sample T-1 at.% (C) Sample U- 2 at.% (d) EDX at 2 at.%

Meanwhile, the X-ray diffraction pattern indicates the crystillinity of undoped ZnO and Sn doped ZnO films as shown in Fig. 2. The XRD pattern indicates the undoped and Sn doped ZnO films exhibited polycrystalline structure with orientation toward c-axis that belongs to the hexagonal wurtzite type (JCPDS #36-1451). There are no peaks corresponding to SnO_2 crystal or other Sn phases were detected from all films. It is observed that the XRD peaks of films were influenced by doping where the peak intensity slightly reduced as the doping concentrations increased. The diffraction peak at (002) of Sample S (undoped ZnO) ,Sample T (Sn doped ZnO-1 at.%), Sample U (Sn doped ZnO-2 at.%) were 34.4, 34.5 and 34.7, respectively. Therefore, shifted of diffraction peak at (002) to a large angle is detected in these Sn doped ZnO films as compared with Sample S (undoped ZnO). Whenever, the Sn concentration increase up to 2 at.% there are more Sn^{4+} is introduced, due to that more influence on ZnO lattice structure such as lattice stress [21]. Ma et. al.[22] reported that the crystallinity of ZnO affected by the grain size. Thus, the crystallinity of ZnO films decreased from 0 at.% to 2 at.% whereby the FESEM results shows the changes of ZnO particle size. In our results, the crystallinity of ZnO films might be also affected by particle size of ZnO films.

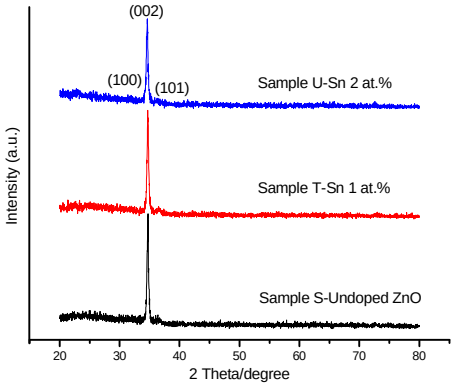

Fig.2. XRD patterns of SZO thin films

The Sn-doped concentration might also affect the electrical properties of ZnO thin film whereby more electron produced whenever Sn concentration increase up to 2 at.%. In order to study the I-V characteristics of ZnO thin films the 2 probes system measurement have been used. Fig. 3 shows the I-V curve of Sn-doped ZnO thin films at applied voltage -10 to 10 V. From this figure, all the thin film shows a good contact with Au as a metal contact. Furthermore, it clearly been seen that ZnO thin film doped at 2 at.% Sn shows the highest current intensity among all Sn-doped ZnO thin films, which reflecting the best of electrical properties, while the undoped ZnO film shows the lowest of current intensity that indicating poor of electrical properties. Moreover, in Fig. 3, the results show the resistivity ZnO thin films decreases as doping concentration increases from 0 at. % to 2 at.% with the lowest of resistivity is 7.7 x 10^2 Ω.cm. Furthermore, the lower of resistivity of Sn-doped thin film from 0 at.% to 2 at.% was due to the successfully of substitutional doping into ZnO structure [23]. Therefore, two free electrons produces from the substitutional doping which increased carrier concentration in the films, that also might affect the electron mobility [24]. This result is similar with the one reported by Chien-Yie et al [25]. Besides that, the grain size for Sample T-Sn 1at.% and sample U-Sn-2at.% was smaller than that undoped ZnO film as estimated from FESEM and XRD results. The smaller of grain size might resulted an increment in the transmission line may be due to a large number of grain boundaries has been generated [20].

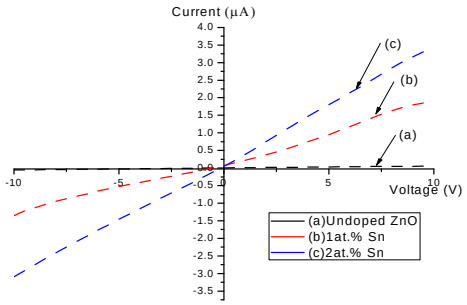

Fig.3. I-V curves of ZnO thin films at Sn concentration: (a) Sample S (b) Sample T (c) Sample U

The transmittance spectra of ZnO films were measured using UV-Vis—NiR spectrophotometer. As depicted in Fig. 4 (a), all the thin films exhibit high transparency more than 90% between visible wavelengths of 400 nm – 800 nm and high absorption edges in UV region. In this study, the transmittance at 2.at% exhibited 96% of average transparency, which was higher than undoped and 1 at.% Sn-doped ZnO thin film. High transmittance of thin film might be due to a small surface roughness of thin film whereby the growth of ZnO was suppressed by Sn dopants and formed flat and fine surfaces [18]. Moreover, the result in this study is comparable and has a slightly higher transmittance from reported by Chien-Yie Tsay *et al*.[25] and Zhanchang Pan *et al*.[26]. Furthermore, high transparency of thin film is useful as a window layer in solar cell application as well as a buffer layer.

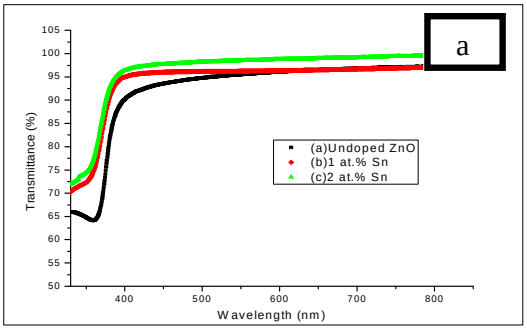

Fig.4. (a) Transmittance and (b) absorption coefficient of the Sn-doped ZnO film

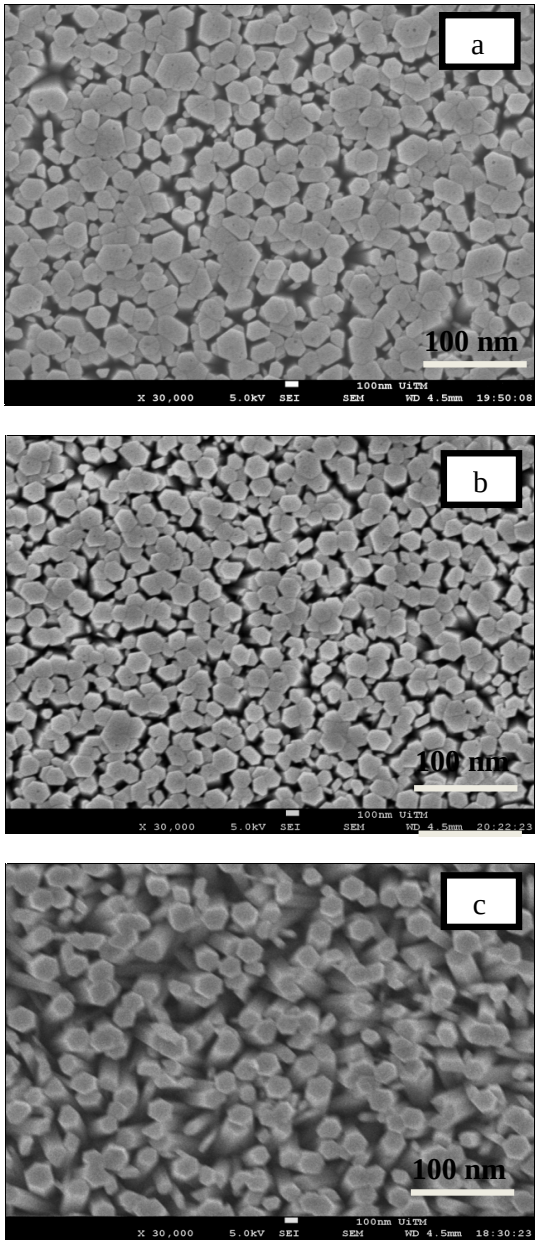

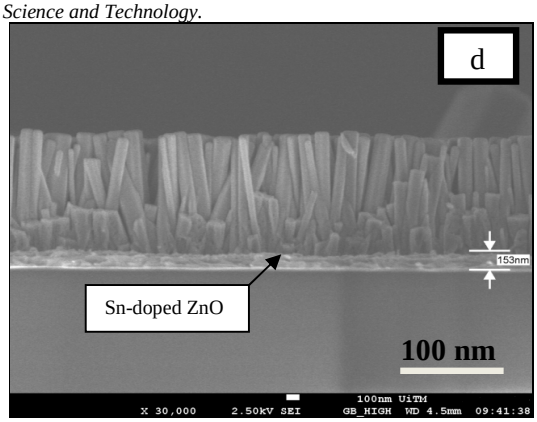

Fig.5. FESEM images of the ZnO nanorods grown on the Sn-doped ZnO seed layer (a) Sample S, (b) on Sample T, and (c) on Sample U (d) Cross-section of ZnO Nanorod

Fig. 5 shows the surface morphologies of ZnO nanorod grown on (0, 1, and 2 at.%) of Sn-doped ZnO thin film. The sample of S, T, and U are employed as the seed layer for the growth of aligned ZnO nanorod. It can be seen that the seed layer with different concentrations of Sn-doped ZnO influenced the morphology and density of ZnO nanorod arrays. The diameter of aligned ZnO nanorod grown on sample U is smaller as compared to both aligned ZnO nanorod grown on sample T and S. This is might be due to the grain size of the seed layer, which can be confirmed by the results on Fig. 1 and also similar as reported by Jin Zhng *et al*[27]. It can be seen that the aligned ZnO Nanorods grown on ITO substrate are crystallized along the ZnO [0001] direction and known as hexagonal prisms that also reported by others [28-29]. Moreover, the aligned ZnO nanorod grown on sample S is the longest as compared to both samples T and U, whereby smaller of nanorods and large interspaces between nanorods indicates the high surface area as shown in Figs.5 and 6.

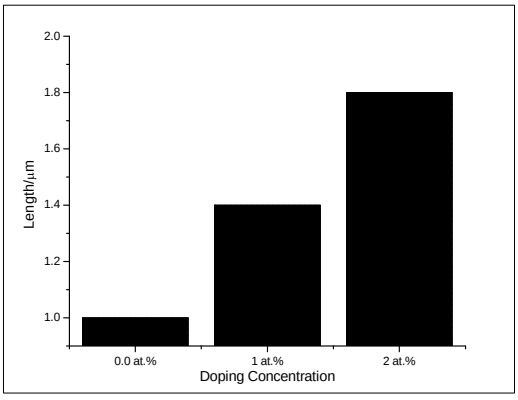

Fig.6. Relationship between the length of the aligned ZnO nanorods arrays and the Sn- doped concentrations

It can be observed that, there are relationship of nanorod growth to the amount of dopents in ZnO thin films, this might be due to high electron concentration at 2 at.% Sn-doped ZnO that helps the growth of aligned ZnO nanorod arrays [28]. Furthermore, the quantity of the grains within the unit area of

sample U is more, as compared to sample S and sample T as can be observed in Fig. 1. In consequences, the larger number of the ZnO nanorod grown on sample with larger interspaces between ZnO nanorod. In addition, the sample U has a smaller grain size leads to a smaller ZnO nanorod growth, while bigger grain size for sample S and T leads to the broader of ZnO nanorod diameter with denser of ZnO nanorod arrays. As discuss earlier, the longest of ZnO nanorod arrays were found on sample U and followed by sample T and sample U. It can be seen that, the bigger the grain size, the shorter of ZnO nanorods arrays. Therefore, it can be concluded that, based on above results and discussion, the aligned ZnO nanorod grown on sample U is suitable for the applications in dye sensitized solar cell. Moreover, the smaller nanorods and large interspaces between nanorods is batter for dye absorption in DSSC application. Meanwhile, Fig.7 shows the transmittance spectra of ZnO nanorod at different Sn-doped ZnO concentrations (0, 1 and 2 at %) seeded layer (no N719 and electrolytes). It can be seen that all nanorod exhibit high transparency of 50-60% between visible wavelengths of 400 nm – 800 nm and the regular wave shape of the transmittance suggests the thickness of ZnO nanorod arrays is uniform, which also confirmed by Fig. 5.

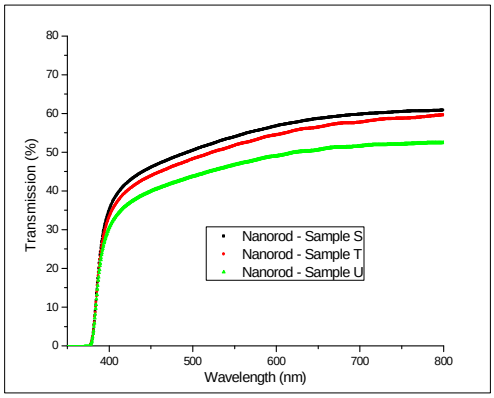

Fig.7. Optical transmittance spectra of ZnO nanorods grown on Sample S, T, and U

The transparency of the ZnO Nanorods for sample S and Sample T is about 60% and 55%. Meanwhile, sample U is about 51%, decreasing of transparency is might be due to surface roughness and verticality of ZnO nanorod. High surface roughness and poor verticality of the ZnO nanorod can caused high light scattering and decrease the transmittance. More importantly, in DSSCs the dye absorption by the films is one of main factor to determine how much the photon energy absorbed from sunlight and transferred as an electric current [30-32].

Fig. 8 shows the I-V characteristics for ZnO Nanorod DSSC grown on the different Sn-doped ZnO concentration. In order to investigate the performances of the solar cells, such as open circuit voltage, (*Voc*), short-circuit density (*Jsc*), fill factor (*FF*) and overall conversion efficiency (η) calculated as:

$$\eta(\%) = \frac{(J_{SC}) \times (V_{OC}) \times FF \times 100\%}{P_{in}} \qquad (2)$$

The aligned ZnO nanorod photoanode (Nanorod Sample U) grown on 2 at% of Sn-doped ZnO film showed higher efficiency as compared to ZnO nanorod photoanode grown on 1 at% and undoped films.

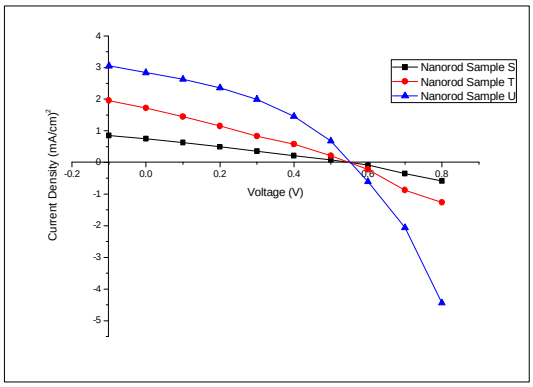

Fig.8 I-V Characteristics of fabricated DSSCs under light density (100mW/cm^2)

It can be concluded that at 2 at% the ZnO nanorod that has large surface area is better than both of ZnO nanorod on the sample T and U, thereby higher of dye absorption in films occurs that contribute to the improvement of DSSCs photovoltaic. Besides that, high density of ZnO nanorod with more pores and also large surface area might enhance the absorption of photon energy from illuminated DSSCs due to high dye absorbed [27-28]. Meanwhile, high density with less pores as well as low surface area might caused low of dye absorption and due to that less of photon generation whenever the DSSCs illuminated thereby proven that the photovoltaic properties of ZnO nanorod photoanode on sample S (Undoped) and Sample T (1 a.%) were lower than Sample U (2 at.% Sn). Table I shows the summarized of photovoltaic performance of DSSCs.

TABLE I PHOTOVOLTAIC PERFORMANCE OF ZNO NANOROD DSSCS FABRICATED ON DIFFERENT SZO FILMS

Photoanode	J_{sc} (mA/cm^2)	V_{oc}	Fill Factor	Efficiency (%)
Nanorod Sample S	0.749	0.528	0.260	0.107
Nanorod Sample T	1.713	0.529	0.265	0.250
Nanorod Sample U	2.320	0.552	0.338	0.599

From these results, the J_{sc}, V_{oc} and energy conversion efficiency η of DSSC increase for the ZnO nanorod photoanode grown at 2 at% Sn-doped ZnO film. It is due to the large surface area of ZnO nanorod thus enriched the absorption of light, which result in higher

absorption of the N719 dye that contribute to high photocurrent density. Other than that, the multi-scattering effect in nanorod may enhance the incident light in them. It is also suggested that, the seeded layer of 2 at.% Sn-doped ZnO thin film which is low resistivity also suitable as a buffer layer whereby reduce the recombination between ZnO nanorod as a photoanode and ITO electrode. Meanwhile, the J_{sc} and V_{oc} for 0 at% and 1 at% of DSSC with ZnO nanorod are smaller as compared to ZnO nanorod on 2 at% Sn-doped ZnO film. Therefore, the compact structure of ZnO nanorod grown on 0 at% and 1 at% films as one a factor that contributes to the lower of J_{sc} and V_{oc} as well as the performance of DSSCs, which is attributed to less absorption of dye and caused of low photon generation due to high recombination occurred at ZnO nanorod surface. Furthermore, the improvement of current density, fill factor and conversion efficiency, for ZnO nanorod grown on 2 at% Sn-doped ZnO film were increased from 0.749 to 2.841, 0.260 to 0.381 and 0.107% to 0.599% respectively, as compared to ZnO nanorod grown on undoped film. The improvement of film quality due to high surface area and higher aspect ratio (width divided by length) of ZnO nanorod on 2 at% Sn-doped ZnO film was proven in this work that contributed to the improvement of DSSCs photovoltaic characteristics.

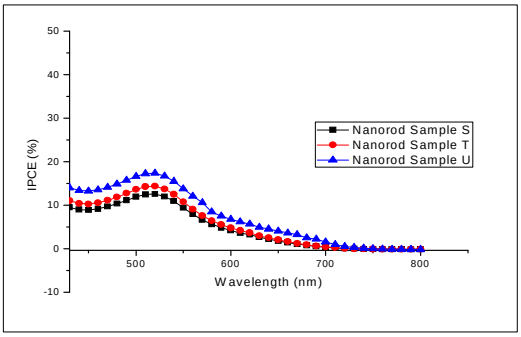

Fig.9. IPCE curve of ZnO Nanorod DSSC grown on Sn-doped ZnO at different concentrations

Fig.9 shows the IPCE of aligned ZnO Nanorod grown on Sn-doped at different concentrations. The IPCE is the ratio of the number of electrons generated by light in the external circuit to the number of incident photons. From Fig. 9, the IPCE of ZnO Nanorod grown at 2 at% sn-doped ZnO thin film is about 18%. Meanwhile, the IPCE of ZnO Nanorod grown on 1 at% and 0 at% Sn-doped are lower than ZnO nanorod grown on 2 at.% Sn-doped ZnO thin film. With better ZnO nanorod growth from 0 at% to 2 at% Sn-doped film the IPCE values increase from 10% up to 18% at 530 nm. This results, confirmed the higher current density for ZnO nanorod grown on sample U. In other hand, the lower of IPCE for these two ZnO nanorod might be due to the ZnO nanorod with less pores and low surface area that contributed to less absorption of dye in films. Moreover, the higher IPCE of ZnO nanorod growth on 2at% Sn-doped ZnO film is attributed to the better dye absorption due to high surface area with more pores of film which can increase the incident light intensity in the N719 dye.

IV CONCLUSIONS

In this study, the effect of Sn-doped ZnO thin films on the structural, optical and electronic properties of ZnO Nanorod were investigated. The surface morphology reveals that the nano-structured ZnO thin films morphologies have a small grain size as a doping concentration increased. The 2 at.% Sn-doped ZnO thin film has a smaller grain size, high transmittance and low resitivity. Moreover, the ZnO nanorods grown on Sn-doped ZnO seed layer has high transmittance in visible region. Furthermore, the ZnO nanorod grown on 2.0 at% Sn-doped ZnO thin film has large surface area with longer aligned ZnO nanorod. Therefore, from the solar simulator measurement under AM 1.5 the improvement of current density, fill factor and conversion efficiency for ZnO nanorod grown on 2 at% SZ0 film were increased from 0.749 to 2.841, 0.260 to 0.381 and 0.107% to 0.599% respectively, as compared to undoped film. With better ZnO nanorod growth from 0 at% to 2 at% Sn-doped film the IPCE values increase from 10% up to 18% at 530 nm. The improvement of film quality due to high density with more pores and length of ZnO Nanorod on 2 at% Sn-doped ZnO film was proven in this work that contributed to the impovement of DSSCs photovoltaic properties. More importantly, the successfully of aligned ZnO nanorod grown on Sn-doped ZnO thin film also can be considered as ones of the contribution in this study.

Acknowledgements

The authors would like to thank the Ministry of Higher Education (MOHE) Malaysia for the financial support, NANO-ElecTronic Centre (NET) and NANO-SciTech Centre of Universiti Teknologi MARA for the facilities.

References:

[1] L. Wang, Y. Kang, X. Liu, S. Zhang, W. Huang, and S. Wang, ZnO nanorod gas sensor or ethanol detection, Sensors and Actuartors B: Chemical. 162 (2012) 237-243.

[2] H. Wang, Z. Wu, Y. Liu, and Z. Sheng, The characterization of ZnO-Anatase-Rutile three components semiconductor and enhanced photocatalytic activity of nitrogen oxides, Journal of Molecular Catalysis A: Chemical. 287 (2008) 176-181.

[3] M. Liao, C M. Liao, C. Hsu, and D. Chen, Preparation and properties of amorphous titania-coated zinc oxide nanoparticles, Journal of Solid State Chemical. 179 (2006) 2020-2026.

[4] A.B. Djuriic, A.M.C. Ng, and X.Y. Chen, ZnO nanostuctures for optoelectronics: Materials and device applications, Progress in Quantum. 34 (2010) 191-259.

[5] D. wei, Dye-sensitized solar cell review, International Journal of Molecular Science. 11 (2010) 1103-1113.

[6] Lung-Chien Chen, Cheng-Chiang Chen, and Bo-Shiang Tseng, Improvement of short-circuit current density in dye-sensitized solar cells using sputterd nanocolumnar TiO_2 compact layer, Journal of Nanomaterials, 2012 (2012) 374052(4pp)

[7] Weiguang Yang, Farong Wan, and Siwei Chen, Hydrothermal

growth and application of ZnO nanowires and TiO_2 buffers in Dye-sensitised solar cells, Nano Research Letter, 4 (2009) 1486-1492.

[8] L. T. Huang, S.R. Huang, M. L. Chang, R.R. Wang, H.C Lin, and M. J. Chen, Dye-sensitized solar cell using ZnO-nanorod electrodes, Journal of Chinese Chemical Society, **58** (2011) 813-816

[9] R. Hatorri and H. Goto, Carrier leakage blocking effect of high temperature sputtered TiO_2 on dye-sensitized solar cells, Journal of Applied Physics, 515 (2007) 8045-8049.

[10] S.H. Hwang, J. Song, Y. Jung, O. Y. Kweon, H. Song, and J. Jang, Electrospun ZnO/TiO_2 composite nanofiber as a bacterial agent, Chemical Communication, 47 (2011) 9164-9166.

[11] D.M. King, X. Liang, C.S. Carney, L.F. Hakim, P. Li, and W. Weimer, Atomic Layer Deposition of UV-Absorbing ZnO Films on SiO_2 Nanoparticles Using a Fluidized Bed Reactor, Advance Functional Materials. 18 (2008) 607-615.

[12] J. Tian, L. Chen, J. Dai, X. Wang, Y. Yin and P. Wu, "Preparation and characterization of TiO_2, ZnO, and TiO_2/ZnO nanofilms via sol-gel process." Ceramics International. 35 (2009) 2261-2270.

[13] Meili Wang, Changgang Huang, Yongge Cao, Qingjiang Yu, Zhaonghua Deng, and Yuan Liu, Dye-sensitized solar cells based on nanoparticle-decorated ZnO/TiO_2 core/shell nanorod arrays, Journal of Physics D: Applied Physics, 42 (2009) 155104 (6pp).

[14] J.F. Chang and M.H. Hon, The effects of of deposition temperature on the properties of Al- doped Zinx oxide thin films, Journal of Thin Solid Films, 386 (2001) 79-86.

[15] G. Jimenez-Cadena, E. Comini, M. Ferroni, A. Vomiero, and G. Sberveglieri, Synthesis of different ZnO nanostrctures by modified PVD process and potential use for 1dye-sensitozed solar cells, Material Chemistry and Physics, 124 (2010) 694-698.

[16] Y.M. Hu, Y.T. Chen, and Z.X Zhang, The morfhology and optical properties of cr-doped ZnO films grown using the magnetron co-sputerring method, Apllied Surfce Science, 254 (2008) 3873-3878.

[17] Sheng Liu, Weiguang Yang, Zhe Hu and Yali Wang, Preparation and characterization of ZnO nanowire arrays grown on different zno seed layers by hydrothermal method, Advance Materials Research, 335-336 (2011) 519-522.

[18] Q. Zhnag, K. Yu, W. Bai, Q. Wang, F. Xu, Z. Zhu, N. Dai, and Y. Sun, Sththesis, optical and field emission properties of three different ZnO nanostrsuctures, Material Letter, 61 (2207) 3890-3892.

[19] C.W. Zou and W. Gao, Fabrication, optoelectronic and photocatalytic properties of some composite oxide nanostructures, Transaction on Electrical and Electronic Materials, 11 (2010) (10pp).

[20] Byeong-Yun Oh, Min-Chang Jeong, Wong Lee and Jae-Min Myong, Properties of transparent conductive ZnO:Al films prepared by co-sputtering, Journal of Cystal Growt, 274 (2005) 453-457.

[21] S. J. Roh, R. S. Mane, S. K. Min, W. J. Lee, C. D Lokhande and S.H. Han, Achievement of 4.51% conversion efficiency using ZnO recombination barrier layer in TiO_2 based dye-sensitized solar cells, Chemistry of Materials, 111 (2007) 8075-8079.

[22] S.F. Wang, T.Y. Tseng, Y.R. Wang, C. Yun. Wang, H.C. Lu, Effect of ZnO seed layers on the solutio chemical growth of ZnO nanorods arrays, Journal of Ceramics International, 35 (2009) 1255-1260.

[23] P.K. Giri, Soumen Dhara, and Ritun Chakraborty, Effect of seed layer on the catalytic growth of vertically aligned ZnO nanorods arrays, Materials Chemistry and Physics, 122 (2010), 18-22.

[24] Maria Arroyo-Hernandez**,** Raquel Alvaro**,** Sheila Serrano, and Jose L Costa-Krämer, Catalytic growth of ZnO nanostructures by rf magnetron sputtering, Nanosacle Research Letters, 6 (2011) 437

[25] Geon Jonn Lee, Soon-Ki Min, Cha-Hwan Oh, Young Pak Lee, Hyunjin Lim, Hyeonsik Cheong, Hyun Jung Nam, Chang Kwon Hwangbo, Sun –Ki Min, and Sung-Hwan Han, Effect od see layers on structural, Morphological, and Optica; properties of ZnO

[26] nanorods, Journal of Nanoscience and Nanotechnology, 11 (2011) 511-517.

[27] Jin Zhang and Wenziu Que: Solar Energy Materials & Solar Cells **94**, (2010) 2186.

[28] Hee Kwan Lee, Myung Sub Kim and Jae Su Yu: Nanotechnology, **22** (2011) 445602.

[29] Xing Tao, Ming Fu, Ailun Zho, Dawei He and Yong Sheng Wang: Journal of Alloys and compounds, **489** (2010) 102.

[30] Ming-Cheng Kao, Hone-Zern Chen, San-Lin Young, Chen-Cheng Lin and Chung-Yuan Kung: Nanoscale Research Letters, **7** (2012) 260.

[31] Weiguang Yang, Farong Wan, Siwei Chen and Chunhua Jing: Nanoscale Research Latter, **4** (2009) 1492.

[32] Yan Feng Gao, Masayuki Nagai, Tien-Chih Chnag and Jing-Jong shyue: Crystal Growth & Design, **7** (2007) 2471.